Drexel University

Annual Progress Report: 2008 Formula Grant

Reporting Period

July 1, 2010 – December 31, 2010

Formula Grant Overview

The Drexel University received $ 1,215,241 in formula funds for the grant award period January 1, 2009 through December 31, 2010. Accomplishments for the reporting period are described below.

Research Project 1: Project Title and Purpose

Triggers of Inflammation in Scleroderma - Scleroderma is a disease caused by uncontrolled accumulation of collagen in the soft tissues. Its cause is unknown and the progression of the disease is not well understood. Recent research has identified a new inflammatory pathway that does not reflect traditional T cell activation. This pathway senses danger signals from the tissues that are external to the cells. The goal of this project is to understand the role of this new inflammatory pathway and other inflammatory signaling pathways in early scleroderma skin lesions and to investigate the signaling in several mouse models that have had pertinent proteins in this new pathway deleted.

Duration of Project

1/1/2009 - 12/31/2009

Summary of Research Completed

This project ended during a prior state fiscal year. For additional information, please refer to the Commonwealth Universal Research Enhancement C.U.R.E. Annual Reports on the Department's Tobacco Settlement/Act 77 web page at http://www.health.state.pa.us/cure.

Research Project 2: Project Title and Purpose

Developing Therapies for Treating Hereditary Spastic Paraplegia - The project goals are to:
1. Identify the deficits in nerve cell shape as well as the transport of substances within nerves when DNA is expressed in the nerve that comprises mutant forms of a protein called spastin that goes awry in a disease called hereditary spastic paraplegia.
2. Test various potential therapies for alleviating these deficits, once identified, in order to provide a basis for the development of new therapies for treating patients with the disease.

Duration of Project

1/1/2009 - 12/31/2009

Summary of Research Completed

This project ended during a prior state fiscal year. For additional information, please refer to the Commonwealth Universal Research Enhancement C.U.R.E. Annual Reports on the Department's Tobacco Settlement/Act 77 web page at http://www.health.state.pa.us/cure.

Research Project 3: Project Title and Purpose

Role of CTF18 in Female Germ Cell Development and Fertility - Infertility is a major medical concern that affects about 1 of every 10 individuals of childbearing age worldwide. Although a significant proportion of infertility is accounted for by identifiable causes, the molecular basis of these defects is often not known or well characterized. Ovulatory dysfunction and diminished ovarian function in infertile women, and low sperm count in infertile men are examples. It is becoming increasingly clear that many more disorders in medicine, including infertility, have a genetic basis than was previously realized. It is our goal to advance the field so that a better understanding of the underlying defects of infertility disorders will lead to improved treatments.

Duration of Project

1/1/2009 - 12/31/2010

Project Overview

Better understanding of the role of *CTF18/Chtf18* in females will broaden our knowledge of the underlying molecular aspects of oogenesis and folliculogenesis, and in doing so will shed light on the underlying defects of infertility in women. Thus, the specific aims of this proposal are:

1. To determine the function of *Chtf18* in mouse oogenesis and folliculogenesis *in vivo*.
Hypothesis: Chtf18 is a critical mediator of oogenesis and folliculogenesis, and its absence causes follicle degeneration. We will assess oocyte and follicle development in ovaries of *Chtf18*$^{-/-}$ and wild-type females using histological criteria and immunofluorescence-microscopy. The underlying cause(s) of a decreased number and aberrant appearance of follicles seen in *Chtf18*-deficient ovaries will be determined. Developmental competency of oocytes and hormonal profiles will also be evaluated.

2. To determine the cause of subfertility in *Chtf18*$^{-/-}$ females.
Hypothesis: Premature separation of homologous chromosomes in meiosis results in aneuploidy and embryonic death leading to significantly impaired fertility. Oocytes will be studied immunocytologically for chromosome segregation defects and embryos will be evaluated for aneuploidy.

Principal Investigator

Karen M. Berkowitz, MD
Assistant Professor
Drexel University College of Medicine
245 N. 15th Street, Mail Stop 495
Philadelphia, PA 19102

Other Participating Researchers

None

Expected Research Outcomes and Benefits

We have generated an experimental system to study CTF18 (known as Chtf18 in the mouse), an evolutionarily conserved gene that is crucial for fertility in the fruitfly and that it is essential for the accurate segregation of chromosomes in yeast. We recently demonstrated that Chtf18 is necessary for fertility and accurate chromosome segregation in the mouse. In addition, almost half of mice lacking Chtf18 die during embryonic development. These data strongly suggest that Chtf18 plays a significant role in normal segregation of chromosomes during development of germ cells (i.e. the cells destined to become eggs and sperm). Defects in these processes are known to contribute greatly to causes of an abnormal chromosome number in offspring, and an abnormal chromosome number often leads to birth defects and/or pregnancy loss. Thus, a better understanding of Chtf18 and its role in germ cell development and chromosomal segregation will shed light on one of the most frequent types of genetic defects that occur during reproduction. Therefore, these studies will provide insight into human infertility and reproductive disorders, ultimately leading to better treatments.

Summary of Research Completed

We generated an experimental system to study *CTF18* (known as *Chtf18* in the mouse), an evolutionarily conserved gene that is crucial for fertility in the fruitfly and that is essential for the accurate segregation of chromosomes in yeast. We recently demonstrated that loss of *Chtf18* in the mouse leads to impaired fertility and chromosomal defects during meiosis. In addition, almost half of mice lacking *Chtf18* die during embryonic development. These data strongly suggest that *Chtf18* plays a significant role in normal segregation of chromosomes during development of germ cells (i.e., the cells destined to become eggs and sperm). Defects in these processes are known to contribute greatly to causes of an abnormal chromosome number in offspring, and an abnormal chromosome number often leads to birth defects and/or pregnancy loss. Thus, a better understanding of *Chtf18* and its role in germ cell development and chromosomal segregation will shed light on one of the most frequent types of genetic defects that occur during reproduction. These studies will provide insight into human infertility and reproductive disorders, ultimately leading to better treatments.

Data collected from each of the following aims (described below) were presented at Drexel University College of Medicine Discovery Day, Philadelphia, PA, October 7, 2010 (first place

for outstanding technician poster).

Specific Aim 1. To determine the function of *Chtf18* in mouse oogenesis and folliculogenesis *in vivo*.

Quantitation of follicle development

We counted ovarian follicles to quantitate the differences observed at different stages of development and scored and categorized follicles as primordial, primary, secondary, and antral according to morphological criteria. Ovarian sections used for histological evaluation were stained with hematoxylin and eosin. Ovaries from *Chtf18*$^{-/-}$and wild-type control females at postnatal days 7 and 21, and at 3 and 6 months of age were collected, processed, paraffin embedded, and counted. We found significantly decreased numbers of primordial follicles at postnatal days 7 and 21 (Figure 1) in *Chtf18*$^{-/-}$ compared with wild-type ovaries. We also found a significant reduction in the numbers of primary, secondary and antral follicles of *Chtf18*$^{-/-}$ ovaries at 3 and 6 months of age (Figure 2). Overall, our data from follicle counts in *Chtf18*$^{-/-}$ ovaries at postnatal days 7 and 21 and at 3 and 6 months of age were statistically significant or trended towards statistical significance (only antral follicle counts of *Chtf18*$^{-/-}$ at 3 months of age), and demonstrated a large size effect, suggesting that these results are biologically relevant. We speculate that antral follicle counts in *Chtf18*$^{-/-}$ ovaries trended toward statistical significance but were not significant because the number of antral follicles in both wild-type and *Chtf18*$^{-/-}$ ovaries were so low. We had proposed counting follicles in females at 9 months of adult age, but we found that follicle numbers were so low and degenerated even in wild-type females that data from this time-point are not meaningful. Our data strongly suggest that *Chtf18* is necessary to maintain the early and developing ovarian follicle pools in female mice, and they indicate that *Chtf18* plays significant roles in mammalian folliculogenesis.

Evaluation of the competency of oocytes.

Oocytes were cultured and allowed to grow and mature *in vitro* in order to assess the developmental competency of *Chtf18*$^{-/-}$ oocytes. Owing to genetic influences of our mouse strain (hybrid of C57BL/6; 129Sv), significant time was required for us to determine and optimize the conditions in which oocytes from our wild-type mice develop and progress. We utilized multiple collection and culture conditions, and we recently found that a significantly greater number of wild-type oocytes progress to meiosis I and II when they are collected in minimum essential medium (MEM alpha medium) and cultured in Chatot Ziomek Bavister (CZB) medium (Figure 3). After determining the optimal culture conditions, we collected data from *Chtf18*$^{-/-}$ female mice and compared it to data from wild-type female mice. We calculated the percentage progression of germinal vesicle–intact oocytes from prophase to metaphase II for *Chtf18*$^{-/-}$ and wild-type mice. Using a Chi square test we analyzed the percentage of GV-intact oocytes reaching metaphase II. We found that 57% of *Chtf18*$^{+/+}$ ooctyes reached metaphase II, whereas only 36% of *Chtf18*$^{-/-}$ ooctyes did so (Figure 3). Due to submendelian ratios our *n* (number of mice per experiment) for *Chtf18*$^{-/-}$ mice was small, so we have continued to collect more data to increase our *n* value.

Specific Aim 2. To determine the cause of subfertility in *Chtf18*$^{-/-}$ females.

Optimization of protocol for evaluation of chromosomes in meiosis.

In order to optimize the number of diplotene nuclei evaluated, we modified our protocol and hypotonic buffers. We confirmed that homologous chromosome pairing and synaptonemal complex formation were normal by examining *Chtf18*$^{-/-}$ chromosomes in oocytes from embryonic ovaries at 17.5 dpc during prophase I (Figure 4). Immunofluorescence microscopy was optimized and performed with rabbit antimouse SYCP1 (Abcam, Inc., Cambridge, UK) and guinea pig anti-mouse-SYCP2 antibodies. We also analyzed surface spread nuclei from oocytes of mice at 18.5 dpc (Figure 4) or postnatal day 0, when the majority of oocytes meiosis has arrested in the diplotene phase of meiosis I. To increase numbers of diplotene nuclei, we also prepared surface spread nuclei from the oocytes of postnatal day 0 and postnatal day 1 pups. Immunofluorescence microscopy was performed (as described above) with rabbit antimouse SYCP3 (Abcam, Inc.), which stains the axial/lateral elements of the synaptonemal complex and human anti-CREST (ImmunoVision, Springdale, AZ), which stains centromeres. We found that the diplotene stage was normal in wild-type females, but we observed four or more univalent chromosomes in 65% (40 nuclei counted) of *Chtf18*$^{-/-}$ females (Figure 4). For studies of metaphase I and metaphase II, oocytes were obtained from the antral follicles of ovaries from 3-week-old eCG-primed females as described above (see "Assessment of the competency of oocytes"). Oocytes were fixed at 16 hours in culture following the first polar body extrusion in order to prepare chromosome spreads at metaphase II. We have begun to evaluate metaphase spreads for congression of chromosomes to the metaphase spindle plate and the distribution of chromosomes along the spindle fibers. We optimized the immunofluorescence and fixation protocols for staining of the meiotic spindle with mouse monoclonal anti-β-tubulin antibody (Sigma, St. Louis, MO) and To-pro-3-iodide, a counterstain to visualize the chromosomes with fluorescence microscopy (Figure 5). Assessment of the results obtained from staining is pending.

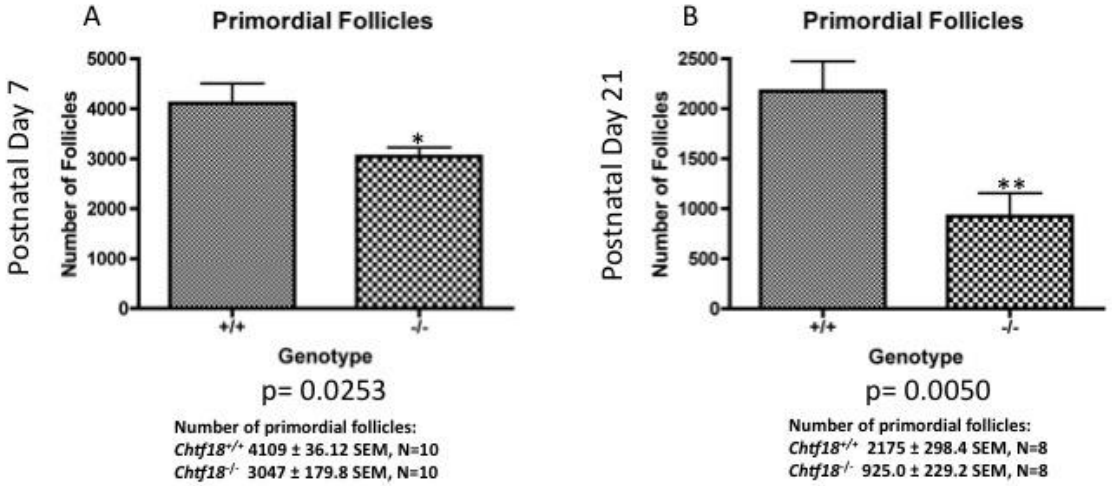

Figure 1. Primordial follicles were significantly decreased in *Chtf18*$^{-/-}$ ovaries at postnatal days 7 (A) and 21 (B).

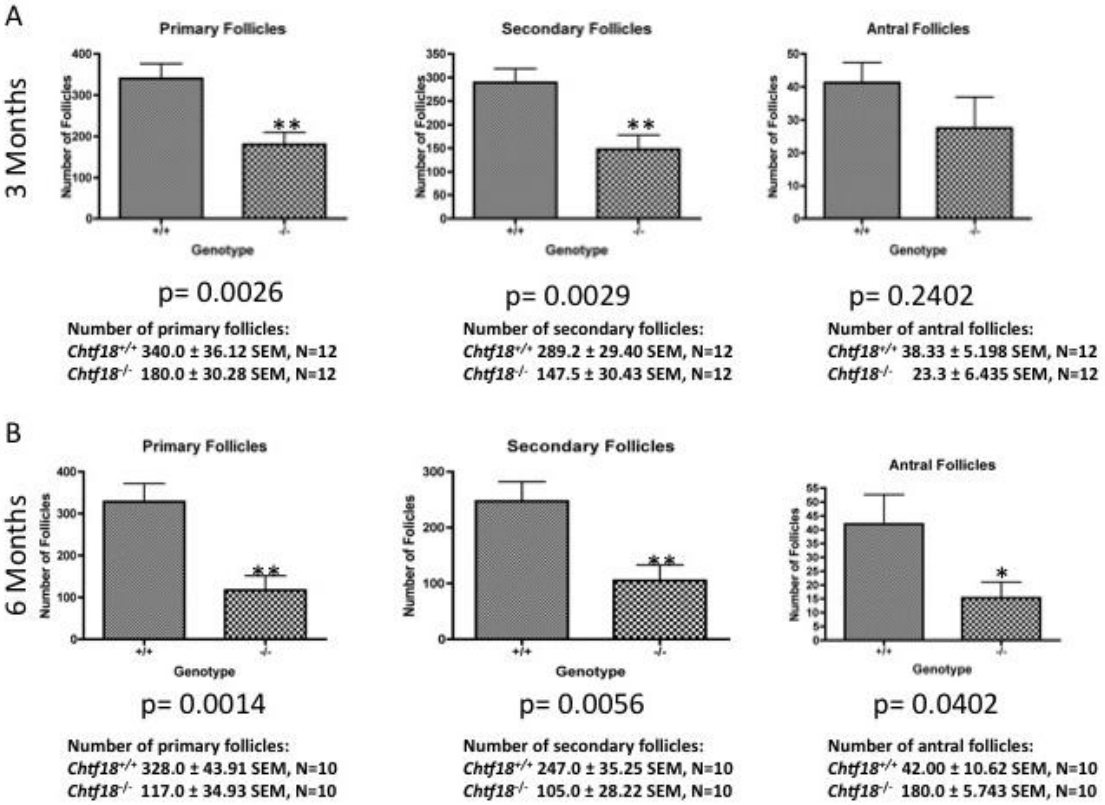

Figure 2. Primary, secondary, and antral follicles were significantly decreased in *Chtf18*$^{-/-}$ ovaries at 3 (A) and 6 (B) months of age.

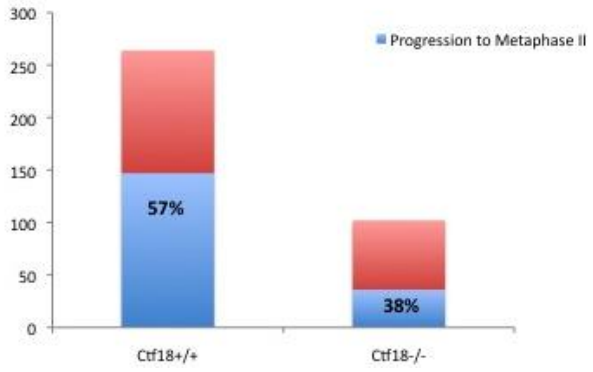

Figure 3. Meiotic progression was significantly impaired in *Chtf18*$^{-/-}$ ooctyes. Percent progression of GV intact oocytes from prophase to MII (metaphase II) was calculated for *Chtf18*$^{+/+}$ control mice and *Chtf18*$^{-/-}$ mice. Statistical comparison was done using Chi-square test to analyze the percentage of GV-intact oocytes reaching MII. Fifty-seven percent of *Chtf18*$^{+/+}$ oocytes reached MII, whereas only 36% of *Chtf18*$^{-/-}$ oocytes reached MII. Using Chi-square test we calculated p = 0.001 (**).

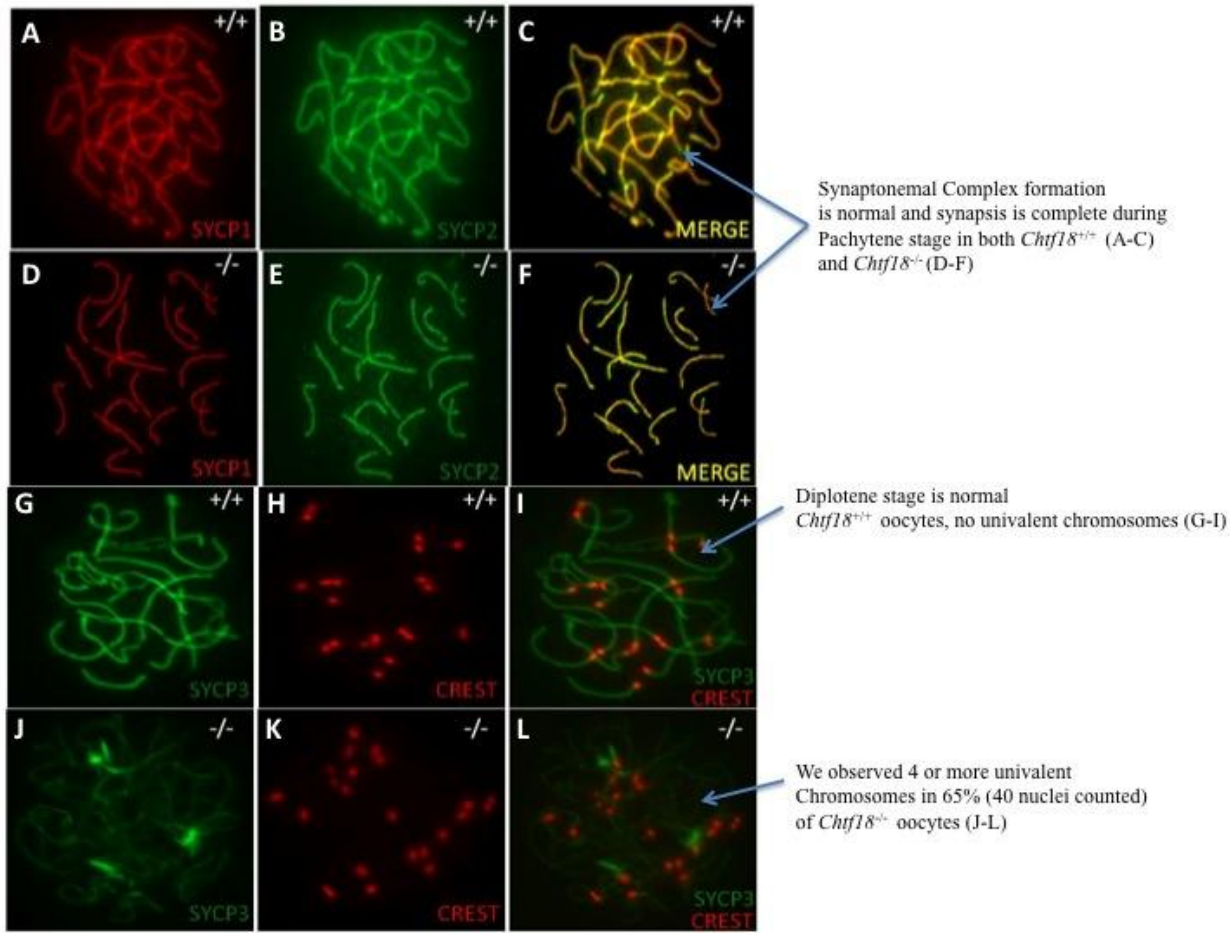

Figure 4. Chromosomes in meiosis. Surface spread nuclei from wild-type (+/+) and *Chtf18*$^{-/-}$ (-/-) oocytes were stained with antisera against SYCP1 (red) and SYCP2 (green) during the pachytene stage of meiotic prophase I (A-F). SYCP1 localizes to central elements of the synaptonemal complex and SYCP2 localizes to the axial/lateral elements of the synaptonemal complex. The merged images (C and F) demonstrate that formation of the synaptonemal complex occurs normally and that synapsis is complete during the pachytene stage in both *Chtf18* $^{+/+}$ (A-C) and Chtf18$^{-/-}$ (D-F) oocytes. Surface spread nuclei from *Chtf18*$^{+/+}$ (+/+) and *Chtf18*$^{-/-}$ (-/-) oocytes were stained with anti-SYCP3 (green), which stains axial/lateral elements of the synaptonemal complex, and anti-CREST (red), which stains centromeres (G-L) during the diplotene stage of meiotic prophase I. Diplotene stage is normal in *Chtf18*$^{+/+}$ oocytes; no univalent chromosomes were present (G-I) as demonstrated by the presence of 20 centromeres per cell. However, we observed four or more univalent chromosomes in 65% (40 nuclei counted) of *Chtf18*$^{-/-}$ oocytes (J-L) as demonstrated by the presence of more than 20 centromeres per cell. Our results suggest that *CTF18* functions to maintain linkage between homologous chromosomes, because synapsis occurs normally but homologues of *Chtf18*$^{-/-}$ oocytes separate prematurely. Using the Mann-Whitney test we calculated p = 0.001 (**).

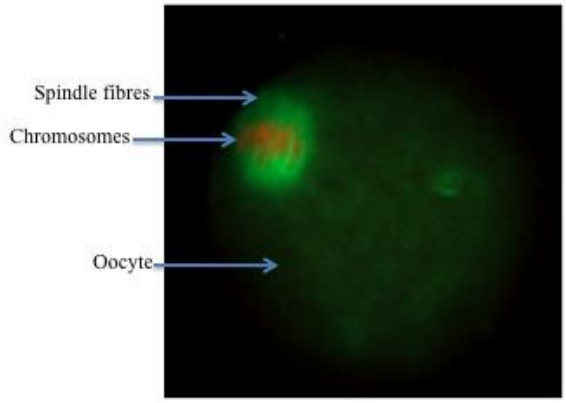

Figure 5. Immunofluorescence staining of a wild-type mouse oocyte with anti-beta-tubulin, which stains the spindle fibers (green), and To-pro-3-iodide, a counter stain which allows visualization of the chromosomes (red) and their alignment on the spindle plate.

Research Project 4: Project Title and Purpose

A Microfluidic Model of Drug-induced Liver Toxicity - Drug-induced liver injury (DILI) is a common reason for terminating drug development, failing to acquire governmental drug approval, or withdrawing a drug from the market. There is no authentic human liver model for predicting DILI in humans. Attempts to make a human liver model have been impeded by the lack of readily available, large quantities of normal human liver cells. A human liver model that retains normal liver architecture and function, while only requiring small numbers of liver cells, is needed. In this project, we will use rat liver cells and fabricated microchannels to produce a mini-liver unit to test DILI. Our long-term goal is to use parameters derived from studies of the rat mini-liver system to generate a human mini-liver system that can be used for human liver biology and DILI studies.

Duration of Project

1/1/2009 - 12/31/2010

Project Overview

The broad objectives and specific aims of this project are: 1). Establish cell growth conditions for layered co-cultures of primary rat hepatocytes and liver sinusoid endothelial cells (LSEC) in a microfabricated, microfluidic environment that mimics a basic functional unit of the liver and 2). Determine the cellular responses of LSEC and hepatocytes in this mini-liver system to Ritonavir exposure.

To achieve these goals, recent advances in microfabrication of mini cell-culture chambers, and construction of microfluidic pumps that can control fluid flow within these chambers, will be combined with techniques for isolation and culture of primary hepatocytes and LSEC to generate layered co-cultures of hepatocytes and LSECs in microchannels. Continuous influx of nutrients and removal of waste and bile will be controlled by microfluidic pumps so that this system mimics the normal microenvironment of a liver sinusoid functional unit.

Hepatocytes and LSEC isolated from rats will be used in this project; rats provide an experimentally tractable system for isolating hepatocytes and LSEC and generating the experimental parameters required to maintain these cells in a microfabricated environment. If required, rat livers can also serve as a source of additional liver-specific cells such as Kuppfer or Stellate cells; inclusion of these might be necessary for generating a fully functional mini-liver unit.

Experimental conditions will first be developed that facilitate the long-term maintenance of functional hepatocytes and LSEC; these will include defining both nutrient and fluid exchange requirements. A thin layer of MatrigelTM that mimics the space of Disse will be used to maintain the layering of the cells. Each cell type will be routinely tested in the mini-liver system to ensure that it retains its liver-specific phenotype and functions. Once established, as an initial evaluation of drug-induced liver injury, cells within this mini-liver system will be exposed to Ritonavir, and the consequence to cell viability or functions will be evaluated. Testing the cellular response to Ritonavir will demonstrate how this system can be used to test drug-induced liver injury.

The long-term goal of this project is to use experimental conditions derived from studies of the rat mini-liver model to generate a human mini-liver system that recreates the normal cellular, architectural and fluidic microenvironment of a human liver functional unit and serves as a system for analyses of human liver physiology and drug-induced liver toxicity.

Principal Investigator

Michael J. Bouchard, PhD
Assistant Professor
Drexel University College of Medicine
NCB 11312
Dept. of Biochemistry and Molecular Biology
245 North 15th St.
Philadelphia, PA 19102

Other Participating Researchers

Moses Noh, PhD – employed by Drexel University

Expected Research Outcomes and Benefits

We expect that by combining recent advances in microfabrication and microfluidic technologies with techniques for the isolation and culture of normal hepatocytes and liver sinusoidal endothelial cells (LSEC), we will define conditions for creating layered co-cultures of rat hepatocytes and LSEC that mimic a functional liver unit. These cells will be co-cultured in microchannels, and the final functional unit will only require small numbers of cells. The control of fluid influx and efflux by microfluidic pumps, the maintenance of cellular architecture that is similar to that of a normal liver, and the use of small numbers of cells will create a miniaturized liver unit that can be used to study numerous aspects of liver biology as well as liver responses to

various drugs. While the outlined project will focus on developing this system with rat liver cells, these studies will establish experimental parameters for generating a similar human mini-liver.

The benefit of this research is that it will define conditions required to construct a much-needed human liver system that recreates the normal architecture and environment of the liver while only using small numbers of human liver cells. Human liver cells are usually acquired from surgically removed livers and are limited in availability. In addition, as a proof-of-principle, this rat mini-liver system will be used to study the toxicity of Ritonavir, a drug that is thought to be harmful to the liver. Ultimately, a human mini-liver system can be used to study general liver biology and well as liver-specific responses to drugs. Considering that drug-induced liver injury is the most common reason from removing a drug from the marker, a system that could be used to evaluate this toxicity prior to actual administration to humans would prevent approval of drugs that are potentially toxic to humans.

Summary of Research Completed

At the completion of the prior progress report, we indicated that we have generated a continuous perfusion system in which oxygen and fluids could be delivered to hepatocytes in the microfabricated microchannels (Figure 1). In this system, the microchannels were bonded to a glass surface, which was necessary to prevent fluid leakage from the microchannels; this leakage would be caused by the localized high pressure of the fluid flow. Although primary rat hepatocytes also adhered to the glass surface, viability was less than on collagen-coated tissue culture plate surfaces. We proceeded for the next couple of months to test different coating materials, such as matrigel and collagen, different concentrations of collagen and matrigel, as well as combinations of matrigel and collagen. Additionally, we also tried different coating methods. After numerous attempts, however, we noted that hepatocyte viability was severely impaired in microchannels in which the cell-attachment surface was glass. We then returned to our plastic surfaces with attached microchannels but noted that bonding of the microchannels to plastic was not as resistant to fluid flow as on the glass surfaces, and the microchannels leaked fluid within 24 hours after fluid flow was initiated. At this stage, we decided to take a multi-pronged approach in which we redesigned our procedure for attaching the microchannels to a plastic, collagen-coated surface. Consequently, we began to simultaneously try different methods for bonding the microchannels to plastic while still allowing for efficient collagen coating of the plastic surface. The ultimate goal was to design a new attachment system that could be re-introduced into the continuous perfusion system as well as the dual microchannel platforms. This leakage from the channels was a major impediment to our progress during the final time period of funding and required numerous trial and error strategies. Resolving the leakage issue consumed most of the final months of this funding period. While this process may appear simple, each bonding method and construction process described below required at least 2 to 3 weeks to generate and then an additional 2 to 3 weeks to test; testing required 2 to 3 weeks to ensure that fluid leakage did not develop after prolonged perfusion, which would prevent utilization of this system for studying problems of chronic exposure of hepatocytes to toxins. Our resolution is described below. While resolving the leakage issue, we also continued to fine-tune our hepatocyte and liver sinusoidal isolation and layering procedures and continued to test the impact of flow rates and oxygen concentration on hepatocytes and liver sinusoidal endothelial cells so

that, upon resolving the microchannel leakage problem, all other parameters would be established so that we could assemble our final mini-liver system.

Solving the problem of microchannel leakage: The major impediment to completion of the miniliver system during the final months of funding was leakage from the microchannels attached to plastic surfaces. Although the microchannels bonded to glass could withstand fluid flow rates necessary to maintain hepatocyte viability, glass was not a suitable substrate for longterm attachment and maintenance of viable, differentiated hepatocytes. This forced us to change the substrate that microchannels would be attached to back to plastic for subsequent incorporation into the continuous perfusion system.

We first tried to ascertain the cause of the leakage when microchannels were adhered to a collagen-coated plastic surface. Scanning electron microscopy was used to inspect the surface of the PDMS and collaged-coated petri dishes. However, the results of this inspection were inconclusive. Additionally, we performed a simple experiment to determine if the cells interacting with the edge of the microchannel might contribute to channel leakage in the context of continuous fluid flow. Instead of culturing cells in the PDMS channels laid on a collagen-coated petri dish, only culture media was pipetted into the channels and was changed twice daily to simulate the culture media change routinely performed for the cells. In this experiment, only 1 of 32 channels leaked during a 2-week period, whereas the channels with cells have had around around a 75% leakage rate after a couple of days. These results may suggest that the presence of the cells in the channel could contribute to some of the leakage we have observed. In order to fix this leakage issue while not drastically altering the cell culturing set-up, several different methods were attempted. The first method that was tried was laser machining a poly(methyl methacrylate), or PMMA, plate that could be force-fit into the petri dish on top of the PDMS channels. The idea behind this concept is that with the pressure of the PMMA plate on the PDMS, the channels would be sealed off adequately. Also, the PMMA plate was machined so that there were holes in the plate in the shape of the channels; this allowed for access to the channels and prevented the blockage of oxygen diffusion to the cells. However, due to the flexibility of the petri dish, the pressure of the plate against the walls of the dish caused the bottom of the dish to bend, and the channels were never sealed off properly. Another method that was attempted involved a different method of collagen coating. Instead of collagen coating the entire petri dish, the PDMS channels were first placed on the uncoated dish, which allows for better adhesion. Then collagen was pipetted into the channel, filling it, and the collagen was allowed to settle down and attach in the channel. The collagen in the channel helped provide a seal between the edges of the channel and the dish, and consequently, these channels did not leak. Among 28 channels used in cell culture, none of them leaked after a period of 5 days. However, the cells did not attach in significant numbers in this arrangement; there were only patches of healthy cells. Finally, in order to provide a good seal between the channels and the plate, a spring-loaded mechanism has been generated (Figure 2). One part of the assembly of this mechanism requires that two small plastic pieces be glued to the walls of a collagen-coated petri dish on opposite sides. Also, two PMMA plates must be laser machined, and these two plates are then attached by four springs. Once placed in the petri dish, one plate presses against the channels, and the other plate presses up against the pieces glued to the wall of the petri dish. In this arrangement, the springs are deflected slightly, which provides a force down to the channels, properly sealing them off. As of now, 16 channels have been used for cell culture in this

arrangement, and none of them have experienced leakage. Additionally, since this method requires a similar cell-culturing set-up to one we have had previous success with, it can be incorporated into the previously designed continuous perfusion platform. Although our resolution to the leakage issue occurred at the termination of the current funding, we have continued to assemble the final mini-liver apparatus and are finalizing production of this system.

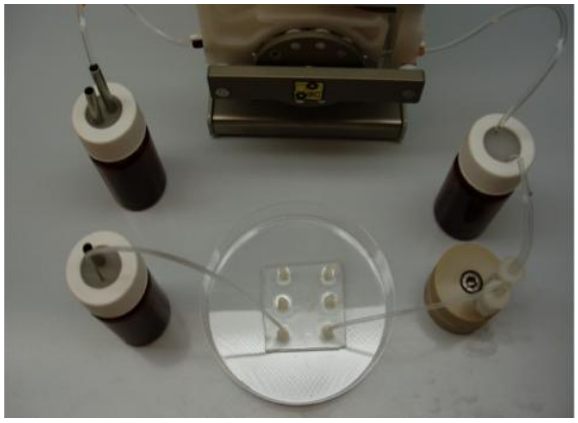

A

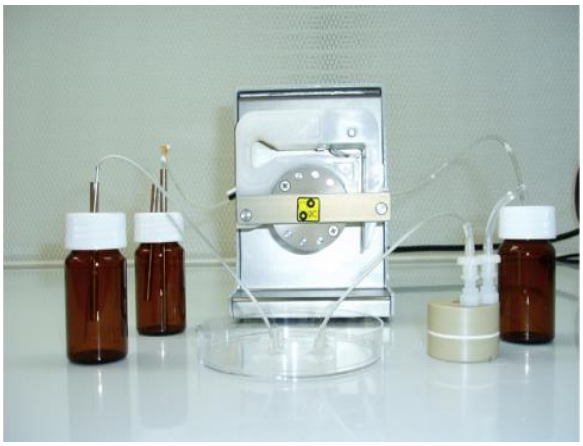

B

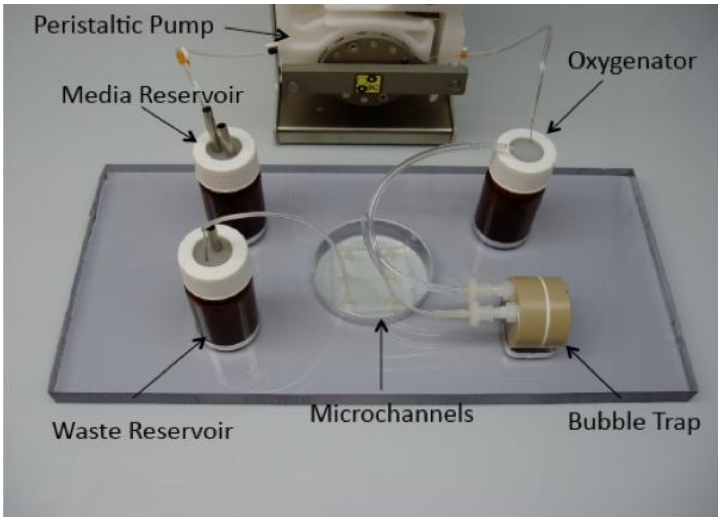

C

Figure 1: Design of dynamic flow system. Panels A and B: dynamic flow system from top and side. Panel C: final system with labeled components. This system is attached to a glass support so that the entire system can be place on the stage of a microscope for continual observation.

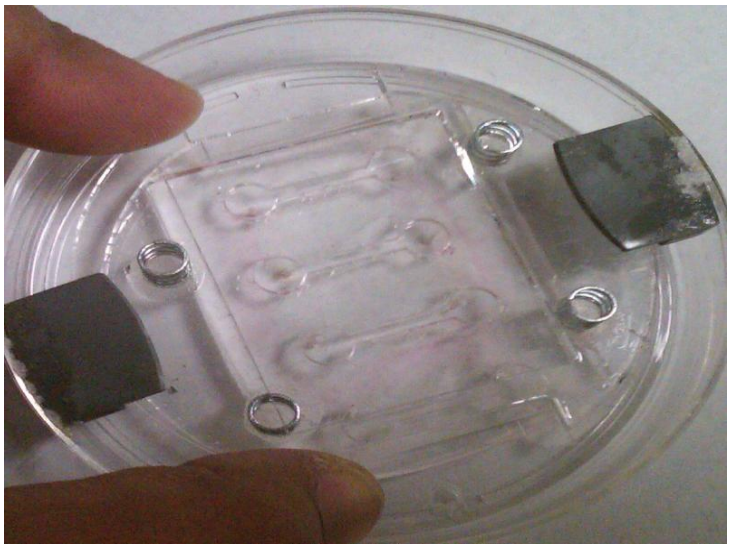

Figure 2: New spring-loaded microchannel device to prevent leakage. See text for details.

Research Project 5: Project Title and Purpose

Identification of Biomarkers and Therapeutic Targets in 3D Hypoxic Breast Cancer Mode - Breast cancer is the most common female cancer in the Western world, affecting 1 of 8 women over their lifetime. One critical prognostic indicator for many tumor types including breast cancer is decreased oxygen levels or hypoxia. Hypoxic cancers are generally associated with aggressive growth, metastasis, and poor response to radiation treatment and chemotherapy. Understanding the molecular mechanisms and signaling pathways driving breast cancer development is critical for developing diagnostic and therapeutic agents. The purpose of this project is to use molecular techniques to analyze the role of hypoxia in regulating gene expression during breast cancer development and to utilize this information to identify novel diagnostic markers and therapeutic targets that can be used to detect and treat breast cancer.

Duration of Project

1/1/2009 - 12/31/2010

Project Overview

The objectives of this project are to characterize the role of hypoxia and to identify the changes in gene expression that promote breast cancer development using a 3D breast cancer model system that we have developed. The overall objective of this grant is to validate and test whether the hypoxia-induced mRNAs that have been identified by microarray analysis are critical for hypoxia-mediated cell survival and the changes in tissue architecture that are observed in our 3D hypoxic model. We have focused on 5 hypoxia up-regulated genes that are likely to be involved with the pathways that lead to the DCIS (ductal carcinoma in situ) phenotype that is observed in 3D hypoxic cultures. We will also test whether targeting these genes reverses the hypoxic survival phenotype and prevents chemoresistance. Additionally, this work will determine whether these target genes can serve as biomarkers for hypoxic breast cancers.

The first aim of this project will use quantitative reverse transcriptase polymerase chain reaction (qRT-PCR) to verify the hypoxia induction of 5 key genes (LOX, ITGA5, MNK2, ET-2, and ANGPTL4) that we identified by microarray analysis. Additionally, immuno-blot analysis will be performed to ensure that changes in RNA levels of these key genes reflect changes in protein expression. The impact of the validated genes on cell survival and DCIS formation in 3D culture will be examined by knocking down the expression of the specific proteins using RNA interference and/or using specific inhibitors (when available).

The second aim of the project will determine if the 5 hypoxia induced genes described in aim 1 are also found in hypoxic DCIS breast cancer patients. We will perform immunohistochemistry (IHC) studies using commercially available tissue arrays to examine whether these 5 are also induced in hypoxic DCIS tumors.

The third aim of this project will determine if the hypoxia mediated changes in gene expression alters sensitivity to chemotherapeutic agents in normal and oncogenic (Her2) expressing breast cancer cells grown in 3D. This aim will be accomplished by treating normal and hypoxic 3D

cultures with the chemotherapeutic agent placitaxel and examining the impact of hypoxia on apoptosis. Additionally, we will examine the impact of the 5 hypoxia induced gene on placitaxel induced apoptosis by knocking out each gene with RNA interference and/or by using specific inhibitors. These studies will aid in identifying novel markers and therapeutic targets to kill hypoxic lesions before they progress to more advanced invasive phenotypes.

Principal Investigator

Gregg J. Johannes, PhD
Assistant Professor
Drexel University College of Medicine
245 N. 15th Street, MS-435
NCB5606
Philadelphia, PA 19102

Other Participating Researchers

Mauricio J. Reginato, PhD, Fernando Garcia, MD - employed by Drexel University College of Medicine

Expected Research Outcomes and Benefits

The anticipated outcome of this project is to validate our 3D breast cancer model and to determine the role of hypoxia in promoting breast cancer development and chemoresistance. We expect to identify new genes and pathways that are critical for the development of breast cancer and that correlate with breast cancer progression. These studies will aid in identifying novel markers and therapeutic targets to kill hypoxic lesions before they progress to more advanced invasive phenotypes. In addition, validating novel pathways or markers in hypoxic human tumors may help guide therapeutic treatment of hypoxic premalignant breast cancers. We will also potentially identify novel therapeutic targets that may reverse hypoxia-mediated chemoresistance. This project will also establish a novel model system to study the role of hypoxia in cancer progression.

Summary of Research Completed

Aim 1: Validate the expression and function of 5 key hypoxia-regulated genes in 3D acini. Over this funding period we used suspension cultures and Bim expression to evaluate the role of the individual target genes on the formation of the DCIS-like structures under hypoxic conditions. The targets analyzed were: Lysyl Oxidase (LOX), Integrin α5 (ITGA5), Map Kinase Interacting Serine/Threonine Kinase 2 (MNK2), and Angiopoietin-like 4 (ANGPL4). We have previously shown that Bim induction is responsible for the induction of apoptosis (Anoikis) and loss of cells in the lumen of 3D MCF10A acini. We have also shown that hypoxia suppresses Bim expression in an Erk dependent manner. This block in anoikis leads to the DCIS phenotype observed in our hypoxic 3D model system. This induction of anoikis can be mimicked by placing cells in suspension and this phenomenon is blocked when cells are grown under hypoxic conditions, similar to what is observed in our 3D model system. Unfortunately none of the tested targets

had any effect on Bim suppression in hypoxic suspension cultures of MCF10A cells. Therefore we concluded that none of the targets had any role in promoting the DCIS phenotype observed when MCF10A cells are grown in 3D conditions under hypoxia (1.0% O_2). We also found that the Endothelin 2 promoter is responsive to hypoxia, even though its sequence does not contain a canonical hypoxia response element (HRE).

Knockdown of the MNK2 or ANGPL4 mRNA does not prevent the hypoxic block in Bim expression. To examine the role of MNK2, we knocked down expression of MNK2 using shRNA#98 and evaluated the impact of hypoxia on Bim expression in cells grown in suspension for 48 hr. As shown in Figure 1, knockdown of MNK2 had no effect on the loss of Bim expression or activation of Erk (measured by Erk phosphorylation) under hypoxic conditions. We did identical experiments to evaluate the impact of ANGPL4 on Bim expression during hypoxia. As shown in Figure 2, the shRNA reduced ANGPL4 mRNA levels by >10-fold (Figure 2A). However this knockdown had no effect on Bim suppression under hypoxic conditions (Figure 2B). We conclude from these experiments that neither MNK2 nor ANGPL4 is involved with the inhibition of apoptosis that allows for the formation of the DCIS phenotype when MCF10A cells are grown in 3D culture under hypoxic conditions.

Inhibition of LOX does not prevent the hypoxic block in Bim expression. To evaluate the role of LOX in the hypoxic block of anoikis mediate by Bim suppression, we used the irreversible LOX inhibitor, β-aminopropionitrile (BAPN). As seen in Figure 3, BAPN treatment had no effect on the loss of Bim expression in MCF10A cells grown under hypoxic conditions in suspension (Figure 3A) or in 3D culture (Figure 3B). Thus we conclude that the induction of LOX by hypoxia had no effect on the inhibition of Bim mediated anoikis that results in the DCIS phenotype observed when 3D MCF10A cultures are exposed to hypoxia.

Knockdown of the ITGA5 mRNA does not prevent the hypoxic block in Bim expression.To test if ITGA5 is involved with the Bim mediated block of anoikis, MCF10A cells were transfected with siRNA targeting this mRNA. As shown in Figure 4, the knockdown of ITGA5 had no effect on the loss of Bim expression in MCF10A cells grown in suspension under hypoxic conditions. This indicates that ITGA5 induction by hypoxia is not involved with the block in anoikis that result in the formation of the DCIS phenotype that occurs when MCF10A cells are grown under hypoxia.

The promoter of the ET2 gene is stimulated by hypoxic treatment. Since it has not been previously reported that ET2 is hypoxia inducible, we analyzed the promoter region for hypoxic response elements. Two overlapping promoter regions of the ET2 gene (-654 to +60, and -459 to +60) were cloned into a promoterless firefly luciferase reporter vector (PGL4, Promega Inc.). The reporter constructs were then transfected into MCF10A cells and the impact of hypoxia on luciferase expression was evaluated. As seen in Figure 5, both constructs showed significant activation when cells were exposed to hypoxia for 48 hr. This indicates that this region of the ET2 promoter contains a hypoxic response element (HRE), although no canonical HRE is observed in the sequence. Considering that ET2 is a HIF2 specific target, the analysis of the ET2 promoter will provide important novel information regarding the cis-acting elements that distinguish HIF1 promoters from HIF2 promoters.

Aim 2: Verify whether the genes identified in hypoxic 3D acini are also altered in hypoxic DCIS tumors. Since none of the tested hypoxic targets showed any biological effect on the hypoxia mediated suppression of Bim (Aim 1), the continued analysis of these targets in Aim 2 and Aim 3 was of limited value. In light of this, we changed Aim 2 to focus on the expression and regulation HIF1 and HIF2 in response to acute and prolonged hypoxia.

New Aim 2: Analysis of the differential regulation of HIF1α and HIF2α in MCF10A cells exposed to hypoxia. We found that the loss of the Hypoxia Inducible Factor (HIF)1α protein correlated with the loss of its mRNA. Additionally, we found the loss of the HIF1α mRNA was a result of a 3-fold reduction in its half-life. This change in half-life correlated with the induction of an endogenous HIF1α anti-sense RNA (aHIF) and a redistribution of the HIF1α mRNA from the nucleus to the cytoplasm.

The loss of the HIF1α protein in response to hypoxia correlates with a reduction in its mRNA. qRT-PCR analysis of the HIF1α and HIF2α mRNAs (Figure 6C) shows that the loss of the HIF1α protein correlates with a >2.5-fold reduction of the HIF1α mRNA. This suggests that the loss of the HIF1α mRNA is responsible for the loss of the HIF1α protein. In contrast the HIF2α mRNA does not significantly change in response to hypoxia.

Hypoxia reduces the half-life of the HIF1α mRNA by 3-fold. To examine the half-life of the HIF1α mRNA in response to hypoxia, the transcriptional inhibitor Actinomycin D (Act D) was added to normoxic cells and cells that have been exposed to hypoxia for 4 hr. Cells were then maintained in their appropriate environments and RNA was harvested after 2, 4, 6 and 8 hr of Act D treatment. As shown in Figure 7A, hypoxia reduced the half-life of the HIF1α mRNA from 30 hr under normoxic conditions to 9.5 hr under hypoxic conditions. This statistically significant 3-fold reduction ($P<0.005$) in half-life is sufficient to account for the loss of the HIF1α mRNA that is observed under hypoxic conditions. The half-life of the HIF2α mRNA was unaffected by hypoxic treatment demonstrating that the reduced stability of the HIF1α mRNA is a specific effect of hypoxia (Figure 7B). In addition we found that this reduction in half-life correlates with the 5- fold induction of the aHIF RNA (data not shown).

The HIF1α mRNA redistributes to the cytoplasm in response to hypoxia. To evaluate if the aHIF RNA or the HIF1α mRNA redistributes from the nucleus to the cytoplasm in response to hypoxia, the amount of the HIF1α mRNA and the aHIF RNA in nuclear and cytoplasmic RNA fractions was determined. Figure 8 shows that the aHIF RNA is 10% cytoplasmic under both normoxic and hypoxic conditions indicating that it does not redistribute during hypoxia. However, the HIF1α mRNA is 20% cytoplasmic under normoxic conditions and 70% cytoplasmic during hypoxia. As expected the cyclophilin A mRNA is 80% cytoplasmic under both conditions verifying the efficient fractionation of the nuclear and cytoplasmic RNA. . This novel finding indicates that the HIF1α mRNA redistributes from the nucleus to the cytoplasm in response to hypoxia. The molecular mechanism responsible for this redistribution and its importance in regulating HIF1α expression remains unknown and is the subject of a grant (RO1, NIH) that will be resubmitted in the near future.

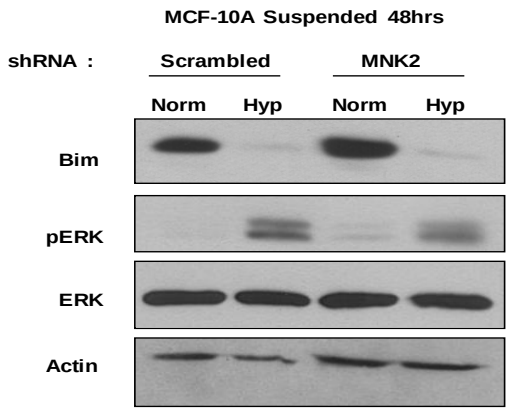

Figure 1. MNK2 induction by hypoxia is not required for the hypoxia-mediated Bim suppression or Erk activation. MCF-10A cells were infected with a lentivirus encoding a scrambled shRNA (scrambled) or one targeting MNK2 (sh #98, MNK2). 48 hours after infection, cells were placed in suspension under normoxic or hypoxic conditions. Immuno-blot analysis was used to determine levels of Bim, phospho-Erk (pERK), and total Erk. Actin was used as a loading control.

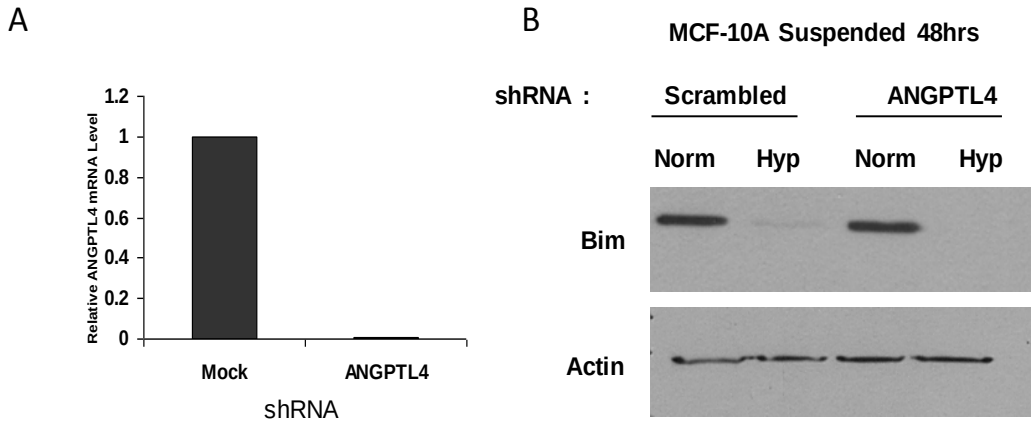

Figure 2. Angiopoietin-like 4 (ANGPL4) expression is not required for hypoxia-mediated Bim suppression. A) MCF-10A cells were infected with a lentivirus encoding a scrambled shRNA (mock) or one targeting ANGPTL4. 48 hours after infection total mRNA was harvested. The amount of ANGPL4 normalized to cyclophilin A was determined by qRT-PCR. The amount of normalized ANGPL4 mRNA found under normoxic conditions was set to 1. B) 48 hours after infection with the ANGPL4 shRNA encoding lentivirus, MCF-10A cells were placed in suspension under normoxic or hypoxic conditions for 48 hours. Immuno-blot analysis was used to determine levels of Bim. Actin was used as a loading control.

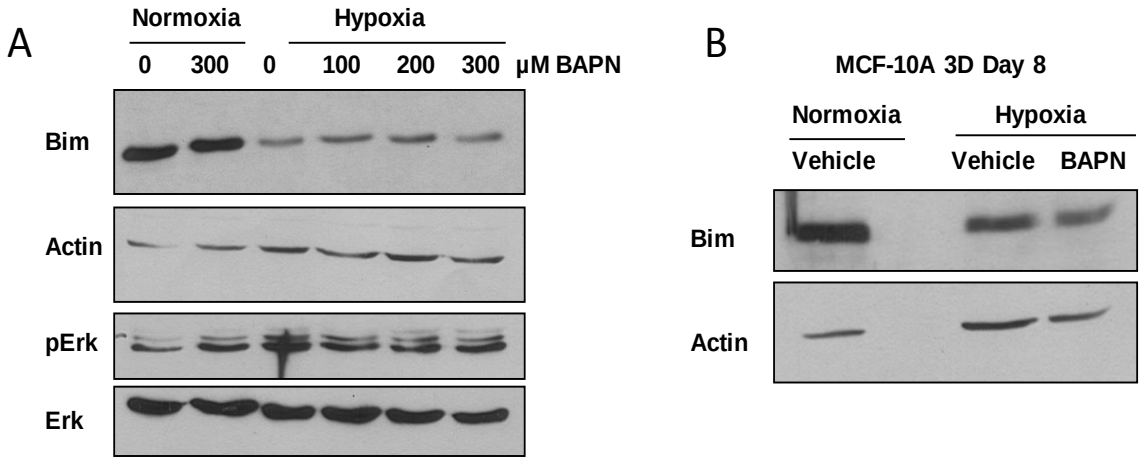

Figure 3. Inhibition of LOX does not reverse hypoxic Bim suppression or Erk activation. A) MCF10A cells were treated with the indicated concentration of the LOX inhibitor β-aminopropionitrile (BAPN) and then placed in suspension for 48 hr under normoxic or hypoxic conditions. Immuno-blot analysis was used to determine the levels of Bim, phospho-Erk (pErk), and total Erk. Actin was used as a loading control. B) MCF10A cells were cultured in 3D until day 6 at which point cells were treated with vehicle (DMSO) or BAPN (300 uM) and then kept under normoxic conditions or placed in hypoxic conditions for 48 hours.

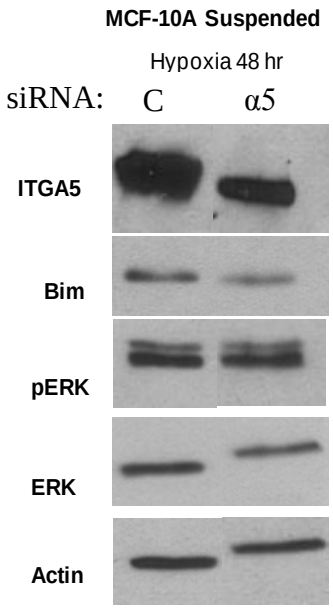

Figure 4. Integrin α is not required for the hypoxia-mediated Bim suppression and Erk activation. MCF-10A cells were mock transfected or transfected with integrin α5-targeting siRNA. 48 hours after transfection, cells were placed in suspension under hypoxic conditions. Immuno-blot analysis was used to determine the levels of integrinα 5, Bim, phospho-Erk (pERK), and total Erk. Actin was used as a loading control. C = mock transfected, α5 = ITGα5

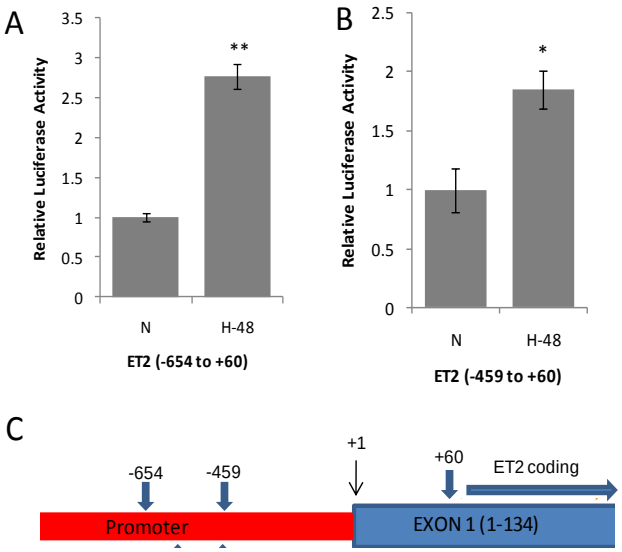

Figure 5. ET2 promoter activity is stimulated by hypoxia. MCF10A cells were transfected with ET2 promoter reporter constructs that contained (A) 650 bp (-654 to +60) or (B) -459 bp (-459 to +60) of the ET2 promoter region. The cells were incubated for 24 hrs and then either maintained under normoxic (N) conditions or placed under hypoxic (H-48) conditions. Cells were harvested and the amount of firefly luciferase (Fluc) activity in the extract was determined using the Dual Luciferase Assay Kit (Promega). All constructs were transfected with a Rennila luciferase control reporter that was used for normalization. The level of normalized Fluc found in normoxic samples was set to 1. Standard error mean bars are shown. *$p \leq 0.05$, **$p \leq 0.005$. C) Schematic representation of the promoter region and first exon of the Endothelin 2 gene. The transcription start site (+1) and the beginning of the ET2 open reading frame is denoted. The location of the forward and reverse primers used to generate the ET2 fragments for cloning into the PGL4.10 (Luc2) plasmid are denoted by arrows.

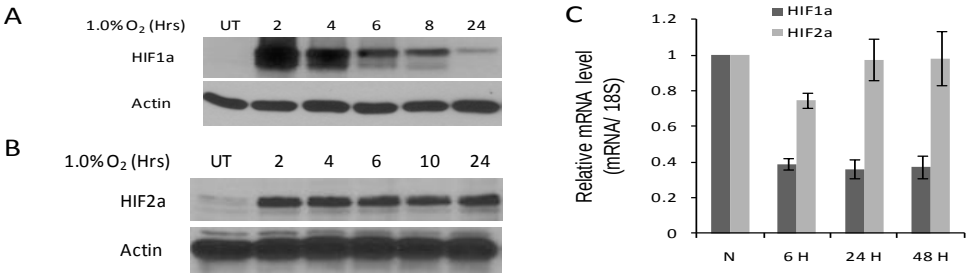

Figure 6. HIF1α is transiently induced by acute hypoxia. MCF10A cells were grown under normoxic conditions (UT) or hypoxic conditions for various times as indicated. A&B) The amount of HIF1α (A) or HIF2α (B) protein was detected by immuno-blot analysis using HIF1α (BD Bioscience) or HIF2α (Novus, Inc) specific antibodies. Actin (antibody from Sigma, Inc) was used as a loading control. C) RNA was isolated from normoxic MCF10A cells or cells that were grown in hypoxia (H) for 6, 24, or 48 hr and the levels of the HIF1α mRNA, HIF2α mRNA, and 18S rRNA was determined by qRT-PCR. All mRNA levels were normalized to 18S rRNA (Relative mRNA level) and the level found under normoxic conditions was set to 1. Standard error bars are shown.

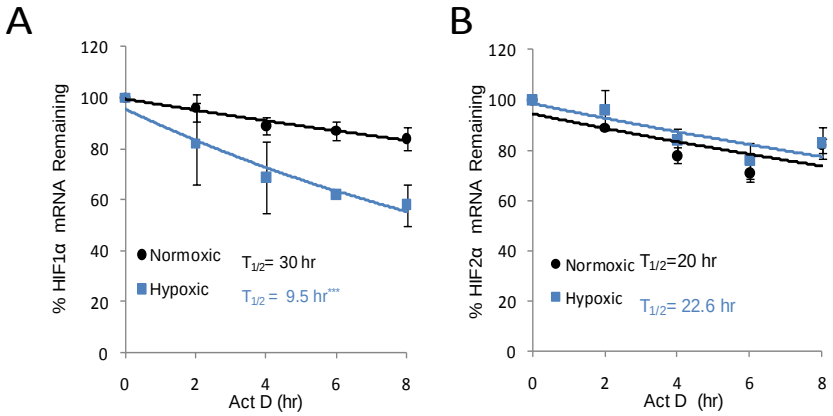

Figure 7. Hypoxia reduces the half-life of the HIF1α mRNA by 3.0-fold. MCF10A cells were grown under normoxic conditions or placed in hypoxia for 4 hr at which point Act D was added and the cells were maintained in the appropriate environment. RNA was harvested at 0, 2, 4, 6, and 8 hr after Act D addition. The amounts of the HIF1α (A) and HIF2α (B) mRNAs were determined by qRT-PCR. Cyclophilin A was used as a normalization control and the normalized value at 0 hr of Act D addition was set to 100%. A linear scale is used to more clearly show the decay of the long-lived HIF1α and HIF2α mRNAs. The half-life for each RNA was determined using the exponential trend line (shown). SEM bars are shown. ***P<0.005 (N vs. H half-life)

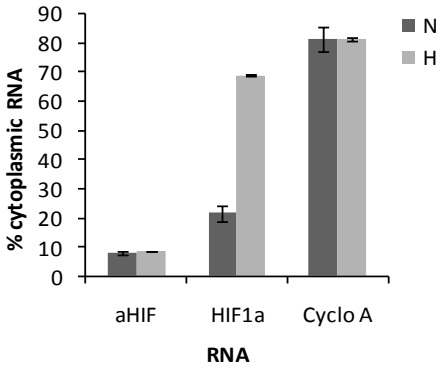

Figure 8. The HIF1α mRNA redistributes from the nucleus to the cytoplasm in response to hypoxic treatment. Nuclear and cytoplasmic RNA was fractionated from MCF10A cells grown under normoxic (N) or hypoxic (H) conditions for 24 hr. The amount of aHIF RNA, HIF1α mRNA, and Cyclophilin A (Cyclo A) mRNA in the nuclear and cytoplasmic RNA fractions was analyzed by qRT-PCR and the % cytoplasmic is shown.

Research Project 6: Project Title and Purpose

Role of O-GlcNac Transferase as a Biomarker and Therapeutic Target for Prostate Cancer - In cancer a number of signaling pathways including phosphorylation/dephosphorylation cascades that add or remove phosphate residues are over-activated. Accumulating evidence suggests a less studied protein modification, known as O-GlcNAc (O-linked N-acetylglucosamine) may globally regulate cell growth and death. The role of O-GlcNAc modifications in prostate cancer phenotypes and signaling is not known. Moreover, we hypothesize that targeting enzymes which regulate O-GlcNAc modifications, such as O-GlcNAc transferase (OGT), may be a novel therapeutic treatment for prostate cancer. Using cell biological, chemical, and proteomic approaches, this project will test the novel hypothesis that O-GlcNAc modifications are increased in prostate cancer, they regulate cancer growth, and thus may serve as novel biomarker and therapeutic targets for prostate cancers.

Duration of Project

1/1/2009 - 6/30/2010

Summary of Research Completed

This project ended during a prior state fiscal year. For additional information, please refer to the Commonwealth Universal Research Enhancement C.U.R.E. Annual Reports on the Department's Tobacco Settlement/Act 77 web page at http://www.health.state.pa.us/cure.

Research Project 7: Project Title and Purpose

Piezoelectric Microcantilever Sensors (PEMS) to Detect Methicillin-Resistant Staphylococcus aureus (MRSA) - The purpose of the project is to develop a real-time, highly-sensitive, highly-specific, portable, cost-effective sensor that can be used to detect MRSA in patient samples in the field (doctors' offices, hospitals, university and college infirmaries, and others), leading to an improved treatment outcome measured by decreased mortality and morbidity.

Duration of Project

1/1/2009 - 12/31/2010

Project Overview

About 19,000 patients died in US hospitals in 2005 of rapidly progressing MRSA infections, and almost 100,000 developed serious infections … leading to more deaths than to AIDS, tuberculosis and viral hepatitis combined. Blacks, the elderly and males are at highest risk. These tragic consequences of MRSA disease have continued to increase nationally. It is imperative that a rapid, sensitive MRSA detection assay be developed. The translational aspect and long term goal (~3 years) of the project is to develop a real-time, highly-sensitive, highly-specific, portable, cost-effective detection system that can be used for MRSA diagnosis of patient samples in the field, leading to improved treatment outcomes measured by mortality and

morbidity. The short term goal is to develop an antibody-based, bench-top piezoelectric microcantilever sensor (PEMS) to detect MRSA. As part of an effort to fulfill this goal, the project has *2 specific aims*: (1) To acquire appropriate antibody (Immunoglobulin G, abbreviated IgG) specific for whole MRSA, MRSA surface components, and MRSA virulence factors, and (2) To attach the anti-MRSA IgG to the PEMS surface in order to optimize specific detection of well characterized MRSA strains, with high specificity and high sensitivity. Aim 2 will be done by modifying and fine tuning an existing lead magnesium niobate - lead titanate (PMN-PT) PEMS.

In addition to commercially available anti-MRSA antibodies, we will use 3 MRSA strains to raise antibodies, and determine which antibodies have the highest specificity and avidity for MRSA binding. IgG will be tested in Enzyme Linked Immunosorbent Assays (ELISAs) against the immunizing MRSA strains, a panel of MRSA strains, and other relevant bacterial pathogens. Antisera will be raised in rabbits against whole UV-killed MRSA. Anti-MRSA IgG will be immobilized on the organic MPS insulation layer of PMN-PT PEMS via the bi-functional linker Sulfo-SMCC. In addition, MRSA will be targeted by multiple (array) PEMS to improve the sensitivity at very low MRSA concentrations. Different PEMS within the array will be bound with different antibodies, each specific to a particular MRSA target. To determine specificity, anti-MRSA IgG-coated PEMS will be challenged with the immunizing MRSA strain, a panel of additional MRSA clinical isolates, bacterial normal skin flora and other Gram positive and Gram negative bacteria causing skin and soft tissue infections (SSTI).

Principal Investigator

Richard F. Rest, PhD
Professor
Drexel University College of Medicine
Dept of Microbiology and Immunology
2900 W. Queen Lane
Philadelphia, PA 19129

Other Participating Researchers

Wan Shih, PhD - employed by Drexel University

Expected Research Outcomes and Benefits

(i) Successfully acquire antibodies that are specific to MRSA and that bind MRSA but not other bacteria that cause skin or soft tissue infections (SSTI) similar to MRSA. Successfully bind functional anti-MRSA antibodies to the sensor (PEMS) surface and demonstrate that the antibody-coated sensor (MRSA PEMS) recognizes MRSA but not other bacteria that cause SSTI.

(ii) If the above outcomes are accomplished, then we are well on our way to developing a commercial product that can rapidly detect MRSA. Our hypothesis is that more rapid detection

of MRSA infection will lead to more rapid antibacterial treatment and thus decreased morbidity and mortality.

Summary of Research Completed

The Piezoelectric microcantilever sensors (PEMS) was fabricated and placed in a flow cell during detection (Figure 1). The total volume of the flow cell was 1.8 ml. A closed container with a 3 ml volume was used as a reservoir. PBS was circulated through the channel at a rate of about 0.7 ml/min and the frequency of the resonance peak around 680 KHz was monitored until it reached a stable baseline with a resonant frequency change of less than 200 Hz over 30 min.

Lead magnesium niobate-lead titanate (PMN-PT)/Cu piezoelectric microcantilever sensors (PEMS) were fabricated from freestanding PMN-PT films of 8 µm thick. A 15-30 nm thick chromium/gold bonding layer was first deposited on one side of the PMN-PT freestanding film to serve as an electrode for plating. A 2-3 µm thick copper layer was electroplated using a copper plating solution of copper sulfate. A 150-nm thick gold was evaporated on both sides of the film. The PMN-PT/Cu bilayer was then cut to the cantilever shape into 1mm by 2mm rectangular strips using a wire saw (Princeton Scientific Precision, Princeton, NJ). Two wires to the top and bottom electrodes were connected using conductive glue and the PMN-PT/Cu strips were finally glued to a glass slide to form the cantilevers).

We examined the effect of the sintering of the PMN-PT freestanding film on the resonance spectra and the detection performance. By sintering the PMN-PT freestanding film at a higher temperature (1100ºC as opposed to 1000 ºC) with better lead-loss compensation, we were able to achieve well sintered PMN-PT films with a 4-µm grain size (see the insert in Fig. 2). As a result, the resonance peaks were much taller as compared to the spectra of the PEMS used in the earlier MRSA detection. Because of the improved PMN-PT property, we showed in a separate HER2 detection that the concentration limit was improved from >100 pg/ml obtained with PEMS similar to those used in the earlier MRSA to 1 pg/ml. The newly developed sintered PMN-PT film, will now be used to detect MRSA with greater sensitivity. We have shown that controlling the grain size in the PMN-PT to >4µm in size, we can improve the concentration limit by more than two orders of magnitude (Figure 3).

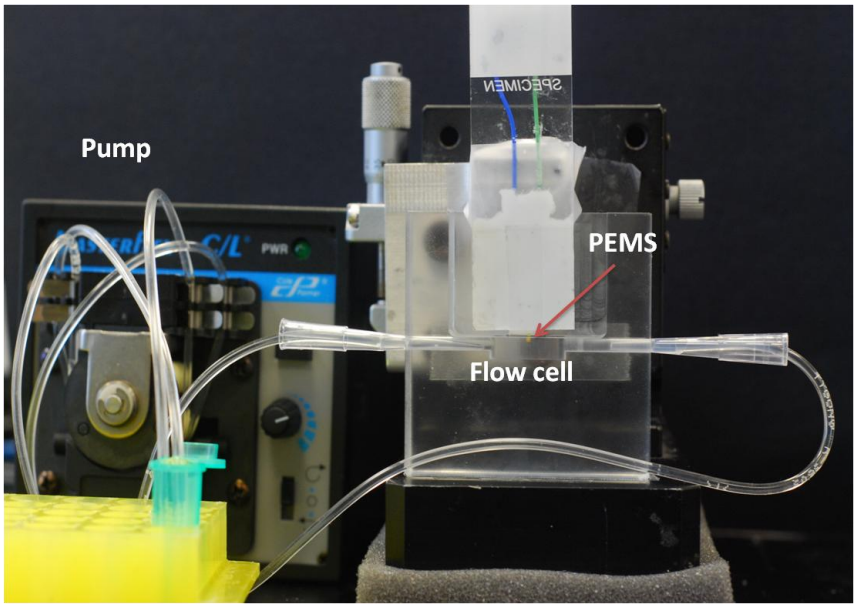

Figure 1: Flow cell set up

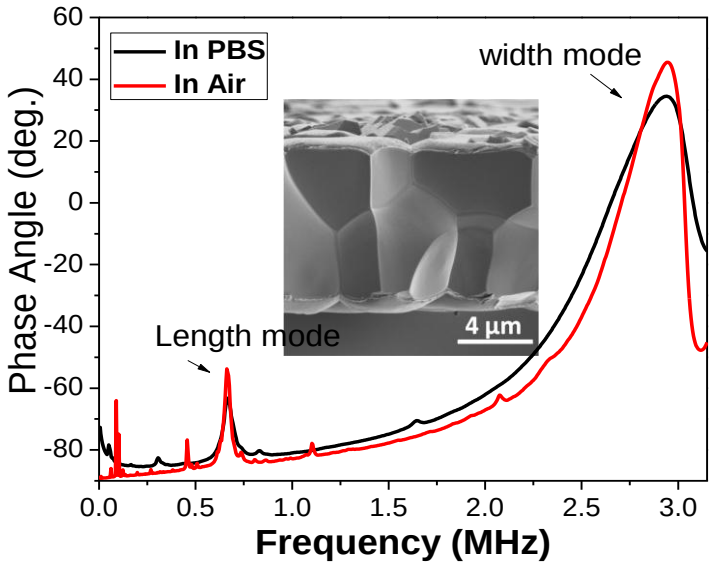

Figure 2**:** In-air and in-liquid resonance spectra of PEMS built with improved PMN-PT freestanding film with a 4 µm grain size.

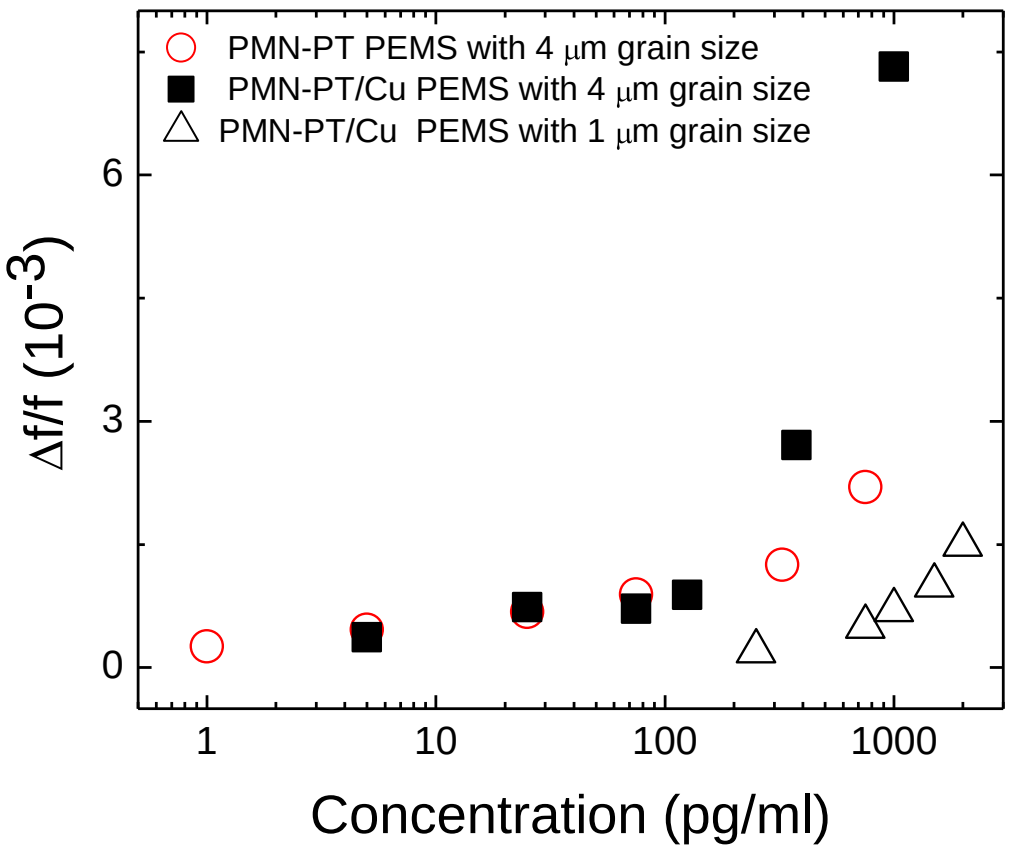

Figure 3: Relative resonance frequency shift Δf/f versus Her2 concentration of PMN-PT PEMS (open circles) and PMN-PT/Cu PEMS (full squares) built with improved PMN-PT freestanding film that had a 4 μm grain size. Also included is the Δf/f versus Her2 concentration of PMN-PT/Cu PEMS (open triangles) built PMN-PT freestanding films that had a 1 μm grain size similar to the PEMS reported in the previous report. As can be seen, the improvement in the PMN-PT freestanding sintering leads to more than two orders of magnitude concentration limit improvement.

Research Project 8: Project Title and Purpose

RNA Interference-based Therapy for HIV-1 Associated Neurologic Disease - The purpose of this project is to lay the foundation for a new method to intervene in the progression of neurologic disease that often develops in HIV-1 infected individuals. We will investigate a method designed to reduce the ability of HIV-1 infected immune cells to migrate into the brain. This migration is enhanced by signals released from brain-resident infected cells in a positive feedback loop that we will disrupt using a strategy based on RNA interference. Certain receptors that are present on the surface of immune cells, and that allow these cells to respond to the migratory signals, will be down-regulated specifically in HIV-1 infected cells. If successful, this will lead to therapies designed to reduce the overall inflammatory immune response to infection in the brain and help to curb the progression of neurologic disorders.

Duration of Project

1/1/2009 - 6/30/2010

Summary of Research Completed

This project ended during a prior state fiscal year. For additional information, please refer to the Commonwealth Universal Research Enhancement C.U.R.E. Annual Reports on the Department's Tobacco Settlement/Act 77 web page at http://www.health.state.pa.us/cure.

Research Project 9: Project Title and Purpose

Somatostatin Signaling in Alzheimer's Disease - A common feature of Alzheimer's disease (AD) is a decrease in the neuropeptide somatostatin in brain. The degree of somatostatin reduction has been correlated with the degree of cognitive decline. However, the role of somatostatin in AD has not been defined. This project is designed to test the function of somatostatin in cognition and cellular models of learning and memory in a mouse model of AD. This project will validate whether somatostatin and its receptors could be utilized as novel therapeutic targets for treating this devastating disease, for which there are currently no effective drugs.

Duration of Project

1/1/2009 - 12/31/2009

Summary of Research Completed

This project ended during a prior state fiscal year. For additional information, please refer to the Commonwealth Universal Research Enhancement C.U.R.E. Annual Reports on the Department's Tobacco Settlement/Act 77 web page at http://www.health.state.pa.us/cure.

Research Project 10: Project Title and Purpose

Characterization and Application of a Novel Drosophila Model for CHARGE Syndrome - The long term goal of this project is a deeper understanding of the pathogenesis of CHARGE Syndrome, a rare autosomal dominant disorder that affects roughly 1 in 10,000 live births. We plan to examine these mechanisms by modeling the disorder in the fruit fly *Drosophila melanogaster*. By creating and validating a working model of CHARGE Syndrome in *Drosophila*, we will be able to genetically test the contribution of candidate genes towards the phenotypes associated with these flies, in order to predict whether these genes may be involved in the symptoms of CHARGE patients. We will also be able to analyze the effect(s) of mutation in these genes on neuronal morphology and connectivity within nerve cells in the fly brain. This approach has been very successful in the past in understanding complex forms of mental retardation.

Duration of Project

1/1/2009 - 12/31/2009

Summary of Research Completed

This project ended during a prior state fiscal year. For additional information, please refer to the Commonwealth Universal Research Enhancement C.U.R.E. Annual Reports on the Department's Tobacco Settlement/Act 77 web page at http://www.health.state.pa.us/cure.

Research Project 11: Project Title and Purpose

Multidimensional Shape/Color Distributions as a Computational Biomarker for Cancer Pathology - The purpose of the project is to develop computational techniques for analyzing histology images of breast cancer tumors. The computational techniques will derive shape and color information from the images that will enable automated evaluation of the tumor. Specifically, the techniques will be used to determine if a patient's breast cancer has spread to nearby lymph nodes by examining a primary tumor that has been removed from the patient. This image analysis capability will eliminate the need for exploratory surgical removal of lymph nodes; thus eliminating the associated side effects, e.g. pain, swelling and morbidity, and costs.

Duration of Project

1/1/2009 - 6/30/2010

Summary of Research Completed

This project ended during a prior state fiscal year. For additional information, please refer to the Commonwealth Universal Research Enhancement C.U.R.E. Annual Reports on the Department's Tobacco Settlement/Act 77 web page at http://www.health.state.pa.us/cure.